Geophysical Research Letters

RESEARCH LETTER
10.1029/2019GL084441

Key Points:
- Limited evaporation from land surfaces poses a major constraint on continental precipitation change, particularly in the Amazon basin
- Warming-induced circulation changes over Africa lead to a decrease in precipitation over South America
- A new simple scaling of precipitation change provides evidence for the impact of circulation anomalies on future rainfall

Supporting Information:
- Supporting Information S1

Correspondence to:
M. Pietschnig,
mp586@exeter.ac.uk

Citation:
Pietschnig, M., Lambert, F. H., Saint-Lu, M., & Vallis, G. K. (2019). The presence of Africa and limited soil moisture contribute to future drying of South America. *Geophysical Research Letters*, *46*. https://doi.org/10.1029/2019GL084441

Received 8 JUL 2019
Accepted 27 OCT 2019
Accepted article online 6 NOV 2019

The Presence of Africa and Limited Soil Moisture Contribute to Future Drying of South America

M. Pietschnig[1], F. H. Lambert[1], M. Saint-Lu[2], and G. K. Vallis[1]

[1]Department of Mathematics, University of Exeter, Exeter, UK, [2]Laboratoire de Météorologie Dynamique/Institut Pierre Simon Laplace, Sorbonne Université, Université Pierre et Marie Curie, Paris, France

Abstract Over oceans, precipitation generally increases with warming in regions where preindustrial precipitation minus evaporation is positive. This simple "wet-get-wetter" principle does not hold over land. The Amazon region and Equatorial Africa currently receive ample rainfall, but the former is projected to dry out whereas precipitation is expected to increase over the latter. Our experiments with an idealized Atmospheric General Circulation Model and realistic continents show that land surface evaporation must be limited in order to obtain drying over the Amazon basin. Our simulations with rectangular, flat continents reveal that large parts of South America would receive more rainfall with warming in the absence of Africa. We suggest that this is due to a warming-induced Matsuno-Gill-type circulation anomaly over Africa. We propose a new simple scaling that diagnoses precipitation change from surface relative humidity change and provides further evidence for the importance of circulation changes for future rainfall.

Plain Language Summary Comprehensive climate models project different precipitation responses to increasing CO_2 levels over land compared to oceans. Maritime precipitation is projected to increase where preindustrial precipitation exceeds evaporation (such as the equatorial regions) and decrease in the subtropical oceans (where evaporation rates exceed rainfall rates). However, continental precipitation change cannot be summarized in such a simplified manner. Equatorial Africa and the Amazon basin both currently see much more rainfall than evaporation, but the Amazon region is projected to dry out in the future, whereas Central Africa will probably receive more rainfall. We find that the drying of the Amazon basin is partly caused by the increase in convection—and thus rainfall—over Equatorial Africa. The ascent of air over Africa leads to subsidence to the west of the continent, resulting in unfavorable conditions for precipitation over tropical South America and the Atlantic Ocean.

1. Introduction

Over oceans and in the zonal mean, preindustrial patterns of precipitation (P) minus evaporation (E) generally become enhanced in a warming climate (Held & Soden, 2006), but this wet-get-wetter scaling does not hold over land (Byrne & O'Gorman, 2015; Chadwick et al., 2013; Roderick et al., 2014). Precipitation change (ΔP) is directly related to $\Delta(P - E)$, because changes in evaporation (ΔE) are relatively uniform (Held & Soden, 2006). We are particularly interested in understanding why the Amazon basin is projected to dry out whereas Equatorial Africa is likely to receive more rainfall in the future (e.g., under the RCP8.5 scenario in the Coupled Model Intercomparison Project-Phase 5 [CMIP5], Taylor et al., 2012, multimodel mean, comparing 1986–2005 to 2081–2100; IPCC, 2013). This response to warming cannot be understood in terms of the wet-get-wetter principle since both regions currently receive ample precipitation.

In contrast to the ocean, E over land does not only depend on the atmospheric moisture demand but also on the availability of water (Manabe, 1969), which is provided by P. As a consequence, $P - E$ cannot be negative over land in the long-term mean (Byrne & O'Gorman, 2015). An initial decrease in P can reduce soil moisture, which leads to a decrease in E that can potentially further reduce precipitation. Hence, in a land-locked region that depends on continental evaporation for precipitation this feedback loop can cause said land region to dry out under global warming. Using an idealized Atmospheric General Circulation Model (AGCM), we show that the parameterization of land surface evaporation must represent soil moisture limitation in order to obtain ΔP patterns similar to those projected by more complex, coupled models.

ΔP cannot solely be understood in terms of changes at the surface, because atmospheric circulation changes play an important role (Chadwick et al., 2013; Chadwick et al., 2016). The Matsuno-Gill theory of the tropical circulation presents a useful framework for understanding those dynamical changes. According to Gill (1980) the tropical continents can be seen as localized surface heat sources which cause convection over the continent and subsidence to the east and west. The relative humidity (r) of sinking air decreases (e.g., Charney, 1975); hence, subsidence regions are associated with dry conditions (Rodwell & Hoskins, 1996), whereas ascent is associated with P. The subsidence to the east of the heat source is associated with a Kelvin wave and surface easterlies and to the west with a Rossby wave and surface westerlies (Gill, 1980). Cook et al. (2004) utilized the Matsuno-Gill theory in order to study the teleconnection between South America and Africa in the present-day climate. The authors showed that, particularly in austral summer, heating over the African continent results in a Walker-type circulation with a subsiding branch over South America. This subsidence suppresses convection and P over the northeastern part of Brazil.

In this study, we employ our idealized atmospheric GCM using a simplified continental configuration with two flat, rectangular continents representing Africa and America in order to study the circulation response to climate forcing. Our results suggest that enhanced convection over Central Africa due to warming suppresses P over the Amazon and subtropical South America in a similar fashion as discussed by Cook et al. (2004). Our results confirm those of Kooperman et al. (2018), who mentioned that the precipitation decrease over the Amazon basin is partly due to the circulation response over Central Africa resulting in subsidence over the region. The idealized nature of our model allows us to test the authors' hypothesis by removing Africa and studying ΔP over America in the absence of this large land mass.

Scaling approaches such as the wet-get-wetter principle yield important insight into the mechanisms which govern tropical precipitation change in complex climate models. If a scaling based on the control conditions and changes in only a few variables is able to capture most of the precipitation change, then that is a strong indication for the importance of those variables in determining future P. Most simple scalings have caveats (as discussed in the respective publications) and therefore do not fully capture ΔP.

Chadwick et al. (2016) and similarly Byrne and O'Gorman (2016) and Rowell and Jones (2006) suggested that warming-induced changes in surface specific humidity (q_S) over land are driven by changes in q_S at the oceanic moisture source for the respective land region. The ocean q_S itself increases approximately by 7%/K following the Clausius-Clapeyron relationship (Held & Soden, 2006). This change in q contributes to the "thermodynamic" component of ΔP, which is the part associated with changes in atmospheric moisture content (Chadwick et al., 2013). This thermodynamic part of ΔP is fairly well understood, whereas changes in the atmospheric circulation (the "dynamic part") are more difficult to diagnose. This has important implications for the skill of these scalings in predicting ΔP, which is sensitive to shifts in the circulation (Chadwick et al., 2016).

We propose a new scaling that links ΔP to the changes in surface relative humidity (Δr_S). Our scaling implicitly includes a dynamical component since changes in the atmospheric circulation influence moisture import and therefore r_S in a region. By applying it in conjunction with the moisture scaling of Chadwick et al. (2016)—which assumes no changes in dynamics beyond a weakening of the circulation—we are able to assess how strongly circulation-driven changes in moisture convergence influence ΔP.

2. Model

Our AGCM experiments are designed using "Isca" (Vallis et al., 2018), a framework for constructing models based on the Geophysical Fluid Dynamics Laboratory system. Isca contains a variety of radiation and convection schemes, continental configurations, and surface properties. In this study, we use the Rapid Radiative Transfer Model (RRTM; Mlawer et al., 1997) and a simplified Betts-Miller convection parameterization (Frierson, 2007). Clouds are currently not represented in Isca, which affects the shortwave component of the atmospheric energy budget.

Evaporation from the ocean surface is parameterized by the bulk formula

$$E_{OC} = \rho \cdot C_D \cdot |\vec{V}| \cdot (q_S^* - q) \tag{1}$$

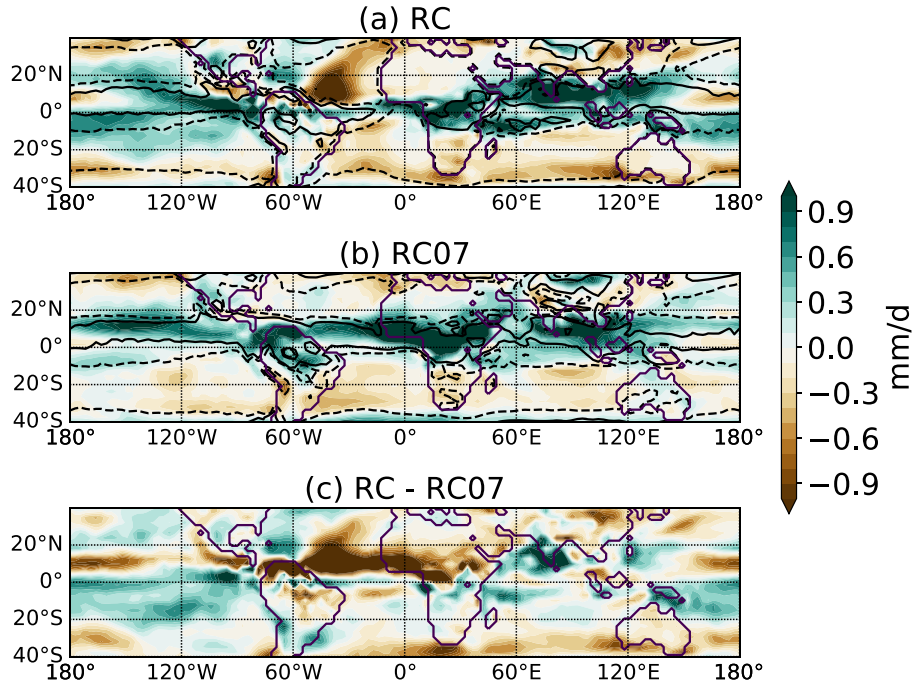

Figure 1. Annual mean ΔP (colors) for RC (a) and RC07 (b), and difference between the two (c). Contours in (a) and (b) show −1.0 (dashed) and 1.0 (solid) $(P-E)_{\mathrm{ctl}}$ in mm/day.

where ρ is the density of the atmosphere, C_D is the drag coefficient which depends on the surface roughness, $|\vec{V}|$ is the magnitude of the velocity, and q is the specific humidity—all in the lowest model layer. The saturation specific humidity at surface temperature is given by q_S^*. Land surface evaporation is parameterized as

$$E_L = C \cdot E_{OC} \tag{2}$$

where C represents moisture conductance by the soil. The simplest approach is to set C to a constant value (e.g., Voigt et al., 2016). This implicitly assumes an infinite supply of moisture, which we find yields unrealistic ΔP (see section 4).

In contrast, the "bucket model" introduced by Manabe (1969) sets C depending on water availability in the soil. Soil moisture increases when P exceeds E until the soil reaches saturation, in which case the excess $P-E$ is treated as runoff. By setting $C = 1$ where soil moisture (W, in meters) exceeds 75% of the field capacity (W_f) and to $C = W/(0.75 \cdot W_f)$ elsewhere, evaporation from the land surface becomes increasingly difficult as the soil dries out. We will show that the parameterization of land surface evaporation based on water availability through the bucket model is required in order to obtain the zonally asymmetric features of tropical precipitation that we are interested in—namely, the drying of northern South America at roughly the same latitude as the P increase over Africa. Our model currently does not include the impact of increasing CO_2 levels on evapotranspiration due to the closure of plant stomata (Sellers et al., 1996) and is therefore likely to underestimate the precipitation response compared to more comprehensive Earth System Models (Skinner et al., 2017; Chadwick et al., 2017).

3. Experiments

We discuss climate change experiments for five different configurations. There are two experiments which use realistic continents and topography (Figure 1) and three with rectangular flat continents (Figure 2). Experiment "RC" has realistic continents with topography, and land evaporation is parameterized with the bucket model. Experiment "RC07" has the same continental configuration, but instead of the bucket model, we set $C = const. = 0.7$ in equation (2). For the idealized continents, we use two flat, rectangular continents representing America and Africa. Rectangular America and Africa span 40° and 60° in longitude, respectively, and cover the entire tropical band in the meridional direction (30°S to 30°N). The rectangular

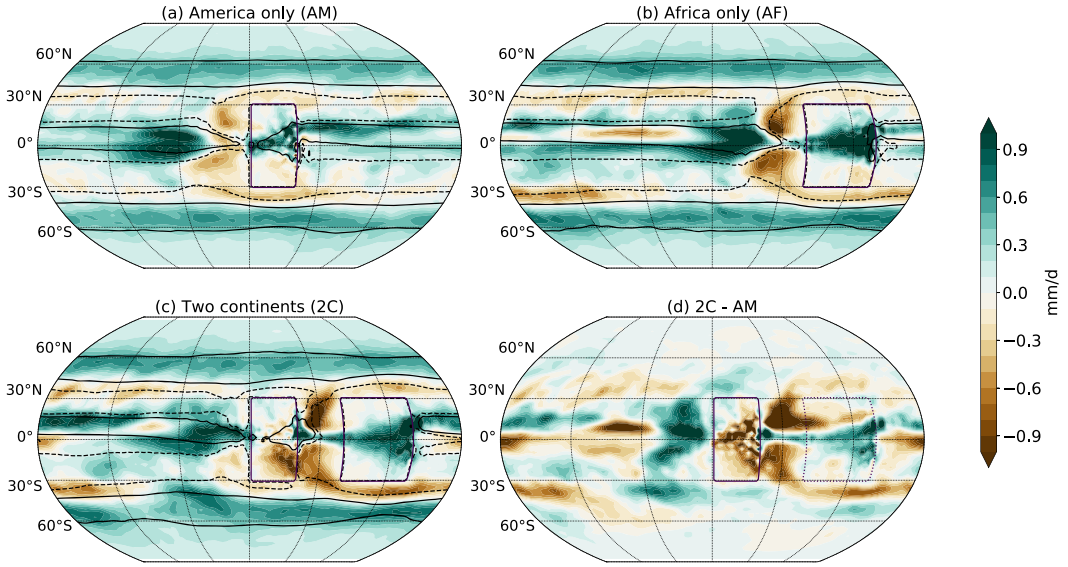

Figure 2. Annual mean ΔP for the idealized experiments: (a) AM, (b) AF and (c) 2C-AM, and the difference between 2C and AM (d). Contours show $(P-E)_{\mathrm{ctl}}$ values of −1.0 (dashed) and 1.0 (solid) mm/day. The purple rectangles show the locations of the idealized continents.

continents are located at a distance of 40° to each other, which is roughly the width of the Atlantic Ocean basin. In experiment "2C" we use both these continents, whereas experiment "AM" and experiment "AF" have only America and only Africa, respectively. In all of the idealized experiments, the bucket model is used. The land albedo is set to 0.33 in all simulations, which is 1.3 times greater than the ocean albedo of 0.25.

For each configuration, a control and a perturbed experiment are run for 40 years each. In the control experiments, a climatology (with seasonal cycle) of zonally uniform sea surface temperatures (SSTs) derived from the Atmospheric Model Intercomparison Project (AMIP, ; Gates, 1992) is prescribed. By using zonally uniform SSTs, the same climatology can be prescribed for the realistic and idealized continents and nonsensical patterns avoided in the latter (Cook et al., 2004). In addition, this approach makes our experiments comparable among each other. Furthermore, for the realistic experiment, precipitation in the control climate (P_{ctl}) and ΔP appear to be relatively insensitive to SST patterns and changes thereof (see supporting information Figure S1).

The climate is perturbed by abruptly doubling CO_2 from 300 to 600 ppmv and imposing a globally uniform ocean warming of 2.52 K. This amount of ocean warming is based on the tropical mean ocean warming in an experiment where the ocean surface is free to respond to CO_2 doubling. Due to the uniform ocean warming, SSTs remain zonally uniform in the perturbed experiments. We choose to force the climate both radiatively and by uniformly increasing SSTs in order to avoid transient shifts of precipitation from land to ocean and vice versa, which would be expected whenever top of atmosphere fluxes are substantially out of balance (Lambert et al., 2011). Differences between the perturbed and control experiment are calculated based on the last 30 years of each experiment (years 10 to 40).

4. The Importance of Soil Moisture

ΔP from our simulation with realistic continents (Figure 1a) qualitatively compares well with the CMIP5 multimodel mean (RCP8.5 scenario, comparing 1986–2005 to 2081–2100; IPCC, 2013). Maritime P increases over the equator and in the midlatitudes and decreases in parts of the subtropics. In the tropical Atlantic to the west of Africa our simulations show a pronounced P decrease which is part of the subtropical precipitation decline (Allen & Ingram, 2002; He & Soden, 2017). Equatorial Africa shows a clear precipitation increase, whereas the response over the Amazon is mixed, with P increasing along the equator and decreasing to the north and south. In the CMIP5 multimodel mean, P generally decreases over the Amazon and increases over Equatorial Africa. These changes mostly do exceed natural variability, but there is no clear agreement among the models on the sign of change (IPCC, 2013). In our simulations, ΔP over Equatorial

Africa is significant, but changes over most of the Amazon do not exceed natural variability (see supporting information Figure S2 and Text S2).

Inourmostrealisticsimulation(*RC*), ΔP roughly follows the wet-get-wetter principle over oceans, that is, positive/negative ΔP coincides with positive/negative $(P-E)_{\mathrm{ctl}}$. In contrast, $(P-E)_{\mathrm{ctl}}$ rates over Equatorial Africa exceed 5 mm/day, and even 9 mm/day in the Amazon basin in our experiment, but ΔP is positive over the former and both negative and positive over the latter. Therefore, ΔP cannot be understood as a simple enhancement of $(P-E)_{\mathrm{ctl}}$ in those regions. However, if land evaporation is not limited by soil moisture (Figure 1b), ΔP is zonally quite uniform and follows the wet-get-wetter principle over ocean and land. Large parts of South America and Africa see a stronger drying in response to warming when soil moisture is limited compared to unlimited evaporation, as shown by Figure 1c. This result suggests that a parameterization of soil moisture is the minimum level of complexity required in order to obtain ΔP projections comparable to Earth System Models.

5. The Influence of Africa on South America

Comparing our simulation with two idealized continents (Figure 2c) to RC (Figure 1a), we find that the patterns of ΔP show a striking similarity between the idealized and realistic experiment. In both simulations, there is a clear P increase over Central Africa and a P decrease over parts of South America. Furthermore, 2C also captures the strong decrease in P over the subtropical Atlantic. The fact that RC and 2C show such similar behavior is an important finding in itself, as it suggests that most of the tropical ΔP is caused simply by the presence of two large land masses at the appropriate distance to each other, and the meridional distribution of SSTs (supporting information Figure S3 shows ΔP in an experiment with a different meridional distribution of SSTs, and supporting information Figure S4 shows ΔP for an experiment similar to 2C but with idealized America extending only to 10°N). Furthermore, the comparability of the ΔP patterns in 2C and RC indicates that studying the idealized continents can shine a light on the more complex, realistic continent experiment and thus help us understand tropical precipitation change in coupled climate models.

Each individual continent experiences an increase in P over the equator (Figure 2a or 2b). However, if both continents are present (Figure 2c), idealized America experiences a widespread decrease in P with warming. The difference between 2C and AM (Figure 2d) shows the influence of idealized Africa on America, namely that drying over America is more widespread due to the presence of Africa compared to AM. This suggests that in the real world, the presence of the African continent has an impact on ΔP over South America. In contrast, the idealized African continent seems to be relatively insensitive to the presence of America (compare Figure 2c to 2b and see supporting information Figure S5). This is in accordance with Cook et al. (2004), who found that—in the present-day climate—the influence of Africa on South America is larger than the other way around. The drying over the Atlantic Ocean also appears to be strongly linked to the presence of Africa, since it is absent in AM.

ΔP over idealized America and the Atlantic Ocean can be better understood when considering changes in the atmospheric circulation (Figure 3). Individually, each continent experiences increased ascent with warming, resulting in anomalous subsidence to the west and east (Figures 3a and 3b). This can be understood as a Matsuno-Gill-type circulation anomaly. Regions of anomalous descent are associated with decreases in r and P. The opposite is true for regions of stronger ascent. In the absence of Africa, idealized America experiences only its own enhancement of ascent and thus an increase in P. When combining the two continents (Figure 3c), the response over Central Africa remains largely unchanged, whereas the convection increase over idealized America is suppressed by the Matsuno-Gill-type circulation anomaly over Africa (Figure 3d and supporting information Figure S6).

Anomalous convection over Africa also leads to subsidence over the Atlantic Ocean in AF and 2C. In addition, there is a decrease in r in the planetary boundary layer over America in 2C which is absent in AM. Warming-induced increases in near-surface q over America and the Atlantic Ocean are also reduced in 2C compared to AM (see supporting information Figure S7). This indicates that dryer air is advected from the region of anomalous subsidence over the Atlantic Ocean onto the American continent. Cook et al. (2004) provided evidence for a similar teleconnection in the present-day climate.

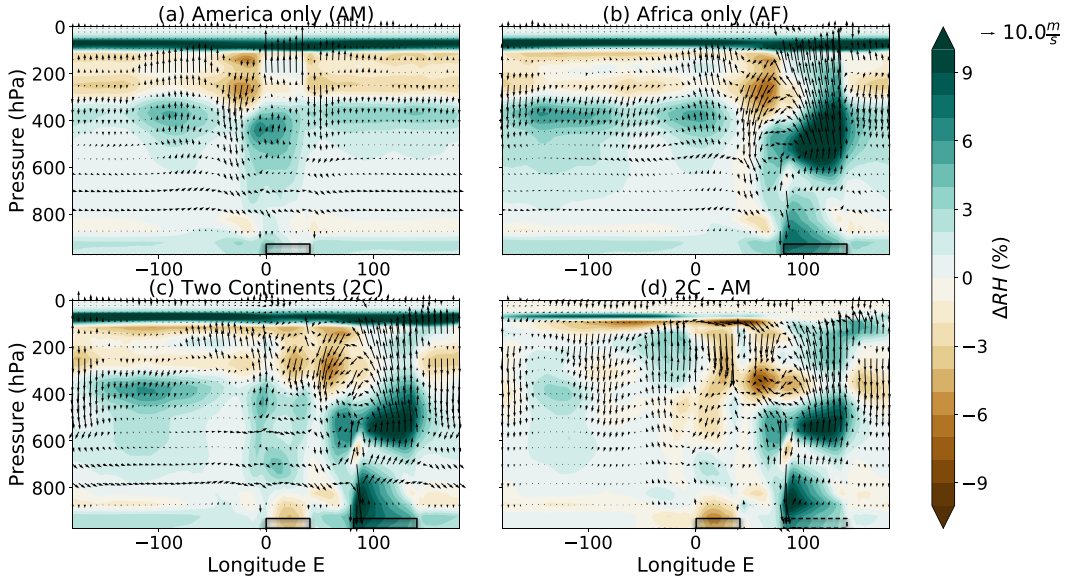

Figure 3. Warming-induced changes in r (colors, in absolute %) and the zonal circulation (vectors, in m/s) averaged over 10°S to 10°N for each idealized experiment: AM (a), AF (b), 2C (c), and the difference between 2C and AM (d). The boxes show the locations of the continents. The change in the vertical velocity has been amplified by a factor of 8,000 following Nie et al. (2010).

6. Simple Scaling of ΔP

Near surface r and temperature (T) are strongly coupled to E and P in our idealized experiments (see supporting information Figure S8). This relationship is particularly marked over land, where r_S, T_S, E, and P are quite well represented as functions of a single variable. This occurs through the role that moist processes play in the surface energy budget. Consider two regions with similar net incoming solar radiation and q at the surface. The first region has high P and therefore plentiful water available for evaporative cooling of the surface. The second region has low P and therefore low E. Incoming radiation must be balanced largely by net upward surface longwave and sensible heat fluxes. As a consequence, T_S is high and r_S is low.

In Appendix A we derive a linearized version of the Lambert et al. (2017) method that associates ΔP with Δr_S over land. ΔP predicted by this method reads as

$$\Delta P_{\text{pred}} = \frac{bP_{\text{ctl}}\Delta T_{S,T} + fP_{T,\text{ctl}}(\Delta r_S - \Delta r_{S,L})}{1 - b\Delta T_{S,T}}. \tag{3}$$

The subscripts T and L stand for tropical mean and tropical land mean, respectively. For example, $\Delta r_{S,L}$ is the change in surface relative humidity averaged over all tropical land regions, but Δr_S is the two-dimensional field of surface relative humidity change. b is the fractional ΔP_T per K warming and $f = \frac{1}{P_{T,\text{ctl}}}\frac{\mathrm{d}P_{\text{ctl}}}{\mathrm{d}r_{S,\text{ctl}}}$, where $\frac{\mathrm{d}P_{\text{ctl}}}{\mathrm{d}r_{S,\text{ctl}}}$ is computed from all tropical land grid points in the control climate. Equation (3) relies on regional differences in Δr_S relative to $\Delta r_{S,L}$ and assumes that the fraction of precipitation that falls over land as opposed to ocean does not change under climate perturbation. Where this assumption is not true, this expression will give biased predictions.

Figure 4a shows the relationship between actual precipitation change (ΔP_{actual}) over land from our 2C experiment and ΔP_{pred} given by equation (3). We find that ΔP_{pred} adequately represents ΔP_{actual}. Mean ΔP_{actual} and ΔP_{pred} are both positive over Africa and negative over America. This suggests that Δr_S and ΔP are indeed coupled over tropical land (equation (3)).

We now explore whether or not these changes would be expected to occur in the absence of changes in the atmospheric circulation. A difficulty is that theoretical expectations for changes in land r_S are not available. However, we can make use of the scaling arguments of Byrne and O'Gorman (2016), Chadwick et al. (2016), and Rowell and Jones (2006) discussed in section 1 to provide estimates of thermodynamic changes in Δq_S and combine these with the control climate relationship between r_S and q_S over tropical land to

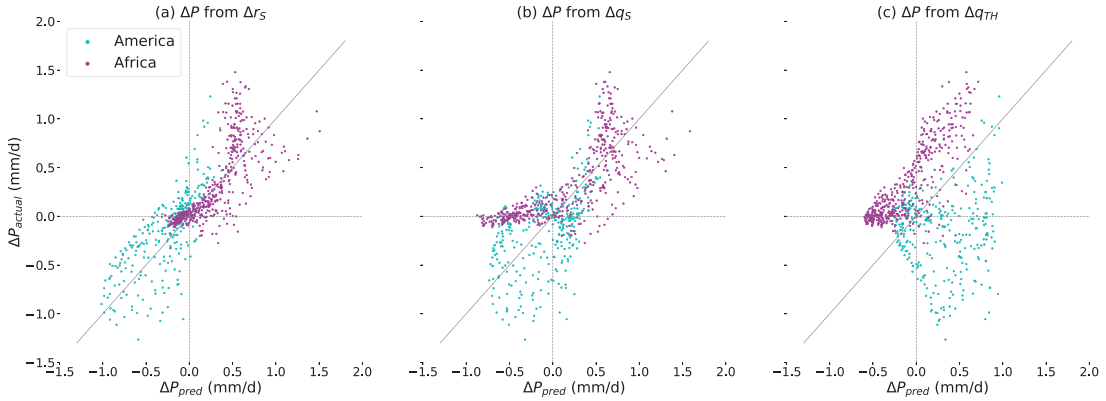

Figure 4. Predicted and actual ΔP (mm/day) for each continent in our 2C experiment. ΔP is predicted from equation (3) in (a), from Δq_S in (b), and from Δq_{TH} in (c). The solid line is $y = x$. Mean changes in precipitation (in mm/day) over America are $\Delta P_{\text{actual}} = -0.1$ and $\Delta P_{\text{pred}} = -0.3$ (a), -0.1 (b), and 0.3 (c). Over Africa, $\Delta P_{\text{actual}} = 0.4$ and $\Delta P_{\text{pred}} = 0.3$ (a), 0.2 (b), and -0.1 (c).

obtain Δr_S (see supporting information Figure S9 and Text S9). Figure 4b demonstrates that ΔP can be predicted competently from actual Δq_S (via Δr_S and equation (3)). In this case, mean ΔP_{pred} is still positive over Africa and negative over America as before. However, if we set Δq_S to be caused by thermodynamic changes alone ($\Delta q_{TH} \simeq \frac{q_{S,\text{ctl}}}{q_{S,T,\text{ctl}}} \Delta q_{S,T}$), then we find that prediction of ΔP is substantially degraded (Figure 4c). Importantly, mean ΔP_{pred} is now negative over Africa and positive over America, opposite to the means of ΔP_{actual}. This suggests that changes in near surface humidity import due to warming—which are not predicted by simple moisture scaling arguments (i.e., Byrne & O'Gorman, 2016; Chadwick et al., 2016; Rowell & Jones, 2006)—are important for ΔP in our 2C experiment.

7. Conclusion

Our study investigates the zonal asymmetry between ΔP over Equatorial Africa and the Amazon basin. Both regions receive ample rainfall in the present-day climate, but the precipitation response is positive over the former and mixed over the latter. This does not follow the simple wet-get-wetter scaling and poses the interesting question of what the different mechanisms are for ΔP in those two regions. We use an idealized AGCM in five different configurations. Two experiments use real-world continents and topography, and three experiments use rectangular, flat continents representing America and Africa.

Despite using an idealized model and zonally uniform SSTs, we obtain ΔP patterns similar to those projected by CMIP5 models if we use realistic continents with the bucket model (Manabe, 1969). In contrast, if evaporation over land is merely reduced by a constant factor compared to ocean evaporation, the P response to warming is zonally uniform. This comparison highlights the importance of including land surface feedbacks between E and P.

Our idealized simulations with two rectangular continents and the bucket model capture most of the ΔP seen in the realistic-continents case. This suggests that the presence of two large land masses is sufficient to capture most of the tropical ΔP projected by complex models. We find that the drying over the Amazon basin and subtropical South America is related to the warming-induced enhancement of convection over Central Africa through the Matsuno-Gill theory. The anomalous ascent over idealized Africa is associated with anomalous subsidence over the Atlantic Ocean and America. This enhanced subsidence suppresses convection and reduces r and, as a result, P in those regions. In the absence of Africa, idealized America receives more rainfall with warming. Our findings support the statement made by Kooperman et al. (2018), that precipitation over the Amazon region is partly reduced due to the circulation response to warming over Central Africa.

Finally, we diagnose ΔP from Δr_S, tropical mean changes in T_S and P_{ctl} only. This simple scaling analysis suggests that dynamical changes in near-surface moisture need to be taken into account in order to reproduce actual precipitation changes. Humidity changes expected from simple thermodynamic scaling are insufficient. Therefore, this analysis provides further evidence for our hypothesis that circulation changes over Africa lead to drying over parts of South America.

Appendix A

Local tropical time mean P can be parameterized as a function of local r_S and T_S relative to the tropical mean (P_T) (Lambert et al., 2017; Todd et al., 2018). In the parameterization, $P = \mathcal{R}(r_S, T_S)P_T$, where $\mathcal{R}$ is a function that relates local r_S and T_S to P relative to P_T. The change in local precipitation amounts between the perturbed (primed) and control climate is then written

$$\Delta P = \mathcal{R}(r'_S, T'_S)P'_T - \mathcal{R}(r_{S,\mathrm{ctl}}, T_{S,\mathrm{ctl}})P_{T,\mathrm{ctl}}, \tag{A1}$$

where it is assumed that $\mathcal{R}$ does not change with climate change.

In our Isca simulations, r_S is close to a single-valued function of T_S over land, meaning that to describe the relative sizes of land precipitation changes, we only need either r_S or T_S. We choose r_S, because the relationship between land P and land r_S is quite linear. Analyzing precipitation over land only, we have

$$\begin{aligned}\Delta P &= \mathcal{R}(r'_S)P'_T - \mathcal{R}(r_{S,\mathrm{ctl}})P_{T,\mathrm{ctl}} + \Delta P_x,\\ \Delta P &= \mathcal{R}(r'_S)\Delta P_T + (\mathcal{R}(r'_S) - \mathcal{R}(r_{S,\mathrm{ctl}}))P_{T,\mathrm{ctl}} + \Delta P_x,\end{aligned} \tag{A2}$$

where $\Delta P_T = P'_T - P_{T,\mathrm{ctl}}$ and ΔP_x describes ΔP due to changes in the fraction of precipitation that falls over land as opposed to ocean. ΔP_x is difficult to calculate in a linear framework because tropical oceanic precipitation amounts are a strong nonlinear function of T_S and tropical oceans show a small range of r_S. Hence, here we assume that $\Delta P_x = 0$ and accept that our estimates will be biased when the fraction of total tropical precipitation that falls over land changes.

We linearize $\mathcal{R}$ changes in terms of $r_{S,L,\mathrm{ctl}}$ as $\mathcal{R}(r'_S) - \mathcal{R}(r_{S,\mathrm{ctl}}) \simeq f \cdot (\Delta r_S - \Delta r_{S,L})$, where f is defined via $\mathcal{R} \simeq f \cdot r_{S,\mathrm{ctl}}$. This provides the second term of equation (A2). For the first term, we notice that $\mathcal{R}(r'_S) = \frac{P'}{P'_T} = \frac{P_{\mathrm{ctl}}+\Delta P}{P_{T,\mathrm{ctl}}+\Delta P_T}$. Substituting these in, we have

$$\begin{aligned}\Delta P &= \left(\frac{P_{\mathrm{ctl}} + \Delta P}{P_{T,\mathrm{ctl}} + \Delta P_T}\right)\Delta P_T + fP_{T,\mathrm{ctl}}(\Delta r_S - \Delta r_{S,L}).\\ \Rightarrow \Delta P &= \frac{bP_{\mathrm{ctl}}\Delta T_{S,T} + fP_{T,\mathrm{ctl}}(\Delta r_S - \Delta r_{S,L})}{1 - b\Delta T_{S,T}},\end{aligned} \tag{A3}$$

where $b = \frac{\Delta P_T}{P'_T \Delta T_{S,T}}$.

Acknowledgments
This study was partly funded by the University of Exeter College of Engineering, Mathematics and Physical Sciences, by NERC (NE/N018486/1), and by the UK-China Research and Innovation Partnership Fund through the Met Office Climate Science for Service Partnership (CSSP) China as part of the Newton Fund. The authors would like to thank Mat Collins for his insightful comments on sea surface temperatures and rainfall, which helped guide the way for the setup used in the present study. Furthermore, Ruth Geen and Stephen Thompson from the Isca modeling group were particularly helpful in solving modeling issues. The data produced for this study are freely available for download on Zenodo: https://doi.org/10.5281/zenodo.3403681 for data used in the main text and https://doi.org/10.5281/zenodo.3403933 for data used in the supporting information.

References

Allen, R., & Ingram, W. J. (2002). Constraints on future changes in climate and the hydrologic cycle. *Nature*, *419*, 228–232. https://doi.org/10.1038/nature01092

Byrne, M. P., & O'Gorman, P. A. (2015). The response of precipitation minus evapotranspiration to climate warming: Why the wet-get-wetter, dry-get-drier scaling does not hold over land. *Journal of Climate*, *28*(20), 8078–8092.

Byrne, M. P., & O'Gorman, P. A. (2016). Understanding decreases in land relative humidity with global warming: Conceptual model and GCM simulations. *Journal of Climate*, *29*(24), 9045–9061. https://doi.org/10.1175/JCLI-D-16-0351.1

Chadwick, R., Boutle, I., & Martin, G. (2013). Spatial patterns of precipitation change in CMIP5: Why the rich do not get richer in the tropics. *Journal of Climate*, *26*(11), 3803–3822. https://doi.org/10.1175/JCLI-D-12-00543.1

Chadwick, R., Douville, H., & Skinner, C. B. (2017). Timeslice experiments for understanding regional climate projections: Applications to the tropical hydrological cycle and European winter circulation. *Climate Dynamics*, *49*(9). https://doi.org/10.1007/s00382-016-3488-6

Chadwick, R., Good, P., & Willett, K. (2016). A simple moisture advection model of specific humidity change over land in response to SST warming. *Journal of Climate*, *29*(21), 7613–7632. https://doi.org/10.1175/JCLI-D-16-0241.1

Charney, J. G. (1975). Dynamics of deserts and drought in the Sahel. *Quarterly Journal of the Royal Meteorological Society*, *101*(428), 193–202. https://doi.org/10.1002/qj.49710142802

Cook, K. H., Hsieh, J-S., & Hagos, S. M. (2004). The Africa–South America intercontinental teleconnection. *Journal of Climate*, *17*(14), 2851–2865. https://doi.org/10.1175/1520-0442(2004)017h2851:TAAITi2.0.CO;2

Frierson, D. M. W. (2007). The dynamics of idealized convection schemes and their effect on the zonally averaged tropical circulation. *Journal of the Atmospheric Sciences*, *64*(6), 1959–1976. https://doi.org/10.1175/JAS3935.1

Gates, W. L. (1992). AMIP: The Atmospheric Model Intercomparison Project. *Bulletin of the American Meteorological Society*, *73*(12), 1962–1970. https://doi.org/10.1175/3801520-0477(1992)073h1962:ATAMIPi2.0.CO;2

Gill, A. E. (1980). Some simple solutions for heat-induced tropical circulation. *Quarterly Journal of the Royal Meteorological Society*, *106*(449), 447–462. https://doi.org/10.1002/qj.49710644905

He, J., & Soden, B. J. (2017). A re-examination of the projected subtropical precipitation decline. *Nature Climate Change*, *7*(11), 53–57. http://doi.org/10.1038/nclimate3157

Held, I. M., & Soden, B. J. (2006). Robust responses of the hydrological cycle to global warming. *Journal of Climate*, *19*(21), 5686–5699. https://doi.org/10.1175/JCLI3990.1

IPCC (2013). Summary for Policymakers. In T. F. Stocker et al. (Eds.), *Climate Change 2013: The Physical Science Basis. Contribution of Working Group I to the Fifth Assessment Report of the Intergovernmental Panel on Climate Change*. Cambridge, United Kingdom and New York, NY, USA: Cambridge University Press.

Kooperman, G. J., Chen, Y., Hoffman, F. M., Koven, C. D., Lindsay, K., Pritchard, M. S., et al. (2018). Forest response to rising CO_2 drives zonally asymmetric rainfall change over tropical land. *Nature Climate Change*, *8*. https://doi.org/10.1038/s41558-018-0144-7

Lambert, F. H., Ferraro, A. J., & Chadwick, R. (2017). Land-ocean shifts in tropical precipitation linked to surface temperature and humidity change. *Journal of Climate*, *30*(12), 4527–4545. https://doi.org/10.1175/JCLI-D-16-0649.1

Lambert, F. H., Webb, M. J., & Joshi, M. M. (2011). The relationship between land–ocean surface temperature contrast and radiative forcing. *Journal of Climate*, *24*(13), 3239–3256. https://doi.org/10.1175/2011JCLI3893.1

Manabe, S. (1969). Climate and the ocean circulation. *Monthly Weather Review*, *97*, 739–774.

Mlawer, E. J., Taubman, S. J., Brown, P. D., Iacono, M. J., & Clough, S. A. (1997). Radiative transfer for inhomogeneous atmospheres: RRTM, a validated correlated-k model for the longwave. *Journal of Geophysical Research*, *102*(D14), 16,663–16,682. https://doi.org/10.1029/97JD00237

Nie, J., Boos, W. R., & Kuang, Z. (2010). Observational evaluation of a convective quasi-equilibrium view of monsoons. *Journal of Climate*, *23*(16), 4416–4428. https://doi.org/10.1175/2010JCLI3505.1

Roderick, M. L., Sun, F., Lim, W. H., & Farquhar, G. D. (2014). A general framework for understanding the response of the water cycle to global warming over land and ocean. *Hydrology and Earth System Sciences*, *18*(5), 1575–1589. https://doi.org/10.5194/hess-18-1575-2014

Rodwell, M. J., & Hoskins, B. J. (1996). Monsoons and the dynamics of deserts. *Quarterly Journal of the Royal Meteorological Society*, *122*(534), 1385–1404. https://doi.org/10.1002/qj.49712253408

Rowell, D. P., & Jones, R. G. (2006). Causes and uncertainty of future summer drying over Europe. *Climate Dynamics*, *27*(2), 281–299. https://doi.org/10.1007/s00382-006-0125-9

Sellers, P. J., Bounoua, L., Collatz, G. J., Randall, D. A., Dazlich, D. A., Los, S. O., et al. (1996). Comparison of radiative and physiological effects of doubled atmospheric CO_2 on climate. *Science*, *271*(5254), 1402–1406. https://doi.org/10.1126/science.271.5254.1402

Skinner, C. B., Poulsen, C. J., Chadwick, R., Diffenbaugh, N. S., & Fiorella, R. P. (2017). The role of plant CO_2 physiological forcing in shaping future daily-scale precipitation. *Journal of Climate*, *30*(7), 2319–2340. https://doi.org/10.1175/JCLI-D-16-0603.1

Taylor, K. E., Stouffer, R. J., & Meehl, G. A. (2012). An overview of CMIP5 and the experiment design. *Bulletin of the American Meteorological Society*, *93*(4), 485–498. https://doi.org/10.1175/BAMS-D-11-00094.1

Todd, A., Collins, M., Lambert, F. H., & Chadwick, R. (2018). Diagnosing ENSO and global warming tropical precipitation shifts using surface relative humidity and temperature. *Journal of Climate*, *31*(4), 1413–1433. https://doi.org/10.1175/JCLI-D-17-0354.1

Vallis, G. K., Colyer, G., Geen, R., Gerber, E., Jucker, M., Maher, P., et al. (2018). Isca, v1.0: A framework for the global modelling of the atmospheres of earth and other planets at varying levels of complexity. *Geoscientific Model Development*, *11*(3), 843–859. https://doi.org/10.5194/gmd-11-843-2018

Voigt, A., Biasutti, M., Scheff, J., Bader, J., Bordoni, S., Codron, F., et al. (2016). The tropical rain belts with an annual cycle and a continent model intercomparison project: TRACMIP. *Journal of Advances in Modeling Earth Systems*, *8*, 1868–1891. https://doi.org/10.1002/2016MS000748